INFECTION AND IMMUNITY, Jan. 2005, p. 546–551 Vol. 73, No. 1
0019-9567/05/$08.00+0 doi:10.1128/IAI.73.1.546–551.2005

Replication Dynamics of *Mycobacterium tuberculosis* in Chronically Infected Mice†

Ernesto J. Muñoz-Elías,‡ Juliano Timm,‡ Tania Botha,§ Wai-Tsing Chan,¶ James E. Gomez, and John D. McKinney*

Laboratory of Infection Biology, The Rockefeller University, New York, New York

Received 30 May 2004/Returned for modification 26 July 2004/Accepted 13 September 2004

The dynamics of host-pathogen interactions have important implications for the design of new antimicrobial agents to treat chronic infections such as tuberculosis (TB), which is notoriously refractory to conventional drug therapy. In the mouse model of TB, an acute phase of exponential bacterial growth in the lungs is followed by a chronic phase characterized by relatively stable numbers of bacteria. This equilibrium could be static, with little ongoing replication, or dynamic, with continuous bacterial multiplication balanced by bacterial killing. A static model predicts a close correspondence between "viable counts" (live bacteria) and "total counts" (live plus dead bacteria) in the lungs over time. A dynamic model predicts the divergence of total counts and viable counts over time due to the accumulation of dead bacteria. Here, viable counts are defined as bacterial CFU enumerated by plating lung homogenates; total counts are defined as bacterial chromosome equivalents (CEQ) enumerated by using quantitative real-time PCR. We show that the viable and total bacterial counts in the lungs of chronically infected mice do not diverge over time. Rapid degradation of dead bacteria is unlikely to account for the stability of bacterial CEQ numbers in the lungs over time, because treatment of mice with isoniazid for 8 weeks led to a marked reduction in the number of CFU without reducing the number of CEQ. These observations support the hypothesis that the stable number of bacterial CFU in the lungs during chronic infection represents a static equilibrium between host and pathogen.

Microbes capable of persisting in their hosts are responsible for some of the most devastating illnesses known to humanity, including hepatitis C, AIDS, malaria, and tuberculosis (TB). Microbial strategies for persistence are highly variable, and the equilibrium established between host and pathogen may manifest itself as a chronic ailment or remain veiled as a subclinical, latent infection with the potential to reactivate later in the lifetime of the host (20, 36).

Following inhalation of *Mycobacterium tuberculosis*, the interplay between an individual's immune response and the infecting bacilli determines whether the infection will lead to active disease or latent TB infection (9). Globally, nearly 2 billion people have been infected with the tubercle bacillus, as estimated from tuberculin skin test surveys, and ~10% of these individuals are expected to develop active TB at some point in their lives (6). TB therapy involves administration of multiple drugs for a minimum of 6 to 9 months; even this prolonged regimen does not always achieve sterilization, as evidenced by posttreatment relapse in a minority of treated individuals (7). The adaptations that allow *M. tuberculosis* to persist in the host despite a vigorous adaptive immune response likely contribute to the difficulty in curing TB with antimicrobial drugs (16, 31).

In the mouse model of TB, a predominantly pulmonary infection can be established after intravenous inoculation or exposure to aerosolized bacteria (21). The acute phase of infection, lasting a few weeks, is marked by exponential growth of the bacterial population in the lungs. The transition to the chronic phase of infection is brought about by the emergence of acquired cell-mediated immunity (CMI), mediated by antigen-specific T cells and macrophage activation, resulting in the stabilization of bacterial numbers in the lungs (10). A longstanding question is whether the plateau in the bacterial growth curve during chronic infection represents a "static" equilibrium, in which bacterial replication is slow or absent, or a "dynamic" equilibrium, in which continued rapid bacterial replication is precisely balanced by an equally rapid rate of killing by the host immune response (27). This issue has important implications for antimycobacterial drug therapy, because drugs that are currently used to treat TB are more effective against bacteria undergoing rapid growth and cell division (17, 19).

In a classic study, Rees and Hart (24) sought to distinguish between "static" and "dynamic" models of the host-pathogen equilibrium in persistent TB by enumerating "viable counts" (CFU) and "total counts" (microscopically detectable acid-fast bacilli [AFB]) in the lungs of chronically infected mice. The authors reasoned that if the dynamic model were correct, the viable counts and total counts should diverge over time due to the progressive accumulation of dead bacilli, which would contribute to the total counts (AFB) but not to the viable counts (CFU). Instead, they found that the viable and total counts were remarkably congruent throughout the course of infection, a result that seemed to favor the static model. They acknowledged, however, that loss of acid-fast staining in dead bacilli

* Corresponding author. Mailing address: Laboratory of Infection Biology, The Rockefeller University, 1230 York Ave., New York, NY 10021. Phone: (212) 327-7081. Fax: (212) 327-7083. E-mail: mckinney@rockefeller.edu.

‡ E.J.M.-E. and J.T. contributed equally to this work.

† This study is dedicated to Philip D'Arcy Hart, whose pioneering research has inspired several generations of TB researchers.

§ Present address: Department of Health Sciences, Faculty of Applied Sciences, Cape Technikon, Cape Town, South Africa.

¶ Present address: Section of Microbial Pathogenesis, Yale University School of Medicine, New Haven, CT 06536.

could result in an underestimate of the true number of total counts. Loss of acid fastness might also explain their observation that the total counts gradually declined in animals treated with the antimycobacterial drug isoniazid (INH), which is known to interfere with acid-fast staining (18). It has also been suggested that acid-fast staining might be lost in tubercle bacilli present in latently infected human tissues (26).

Here we revisited this important aspect of the host-pathogen interface in persistent TB by measuring *M. tuberculosis* viable counts, represented by the number of bacterial CFU, and total counts, represented by the number of bacterial chromosome equivalents (CEQ), in the lungs of chronically infected mice. Our experimentally determined values were compared with values obtained from an in silico model that was used to simulate bacterial growth curves (CFU accumulation) and to predict the extent of accompanying bacterial CEQ accumulation over time at different rates of bacterial cell division. Alternative scenarios in which the immune response was bacteriostatic, bactericidal, or both were modeled. Our results support the static-equilibrium model, in which entry into the chronic phase of infection is accompanied by a marked reduction in the bacterial cell division rate.

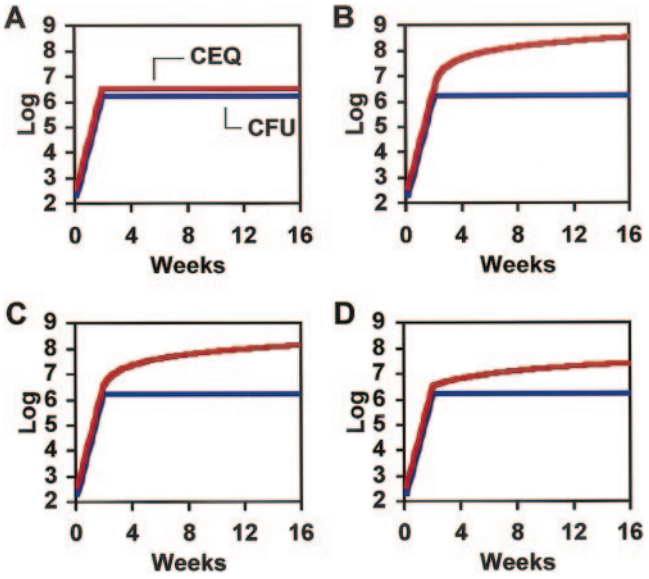

FIG. 1. Modeling static and dynamic scenarios of the host-pathogen equilibrium in chronic murine TB. Mice are infected with 200 CFU. Acute-phase infection (0 to 2 weeks) is characterized by an exponential increase in viable counts (CFU), with a 24.6-h population doubling time. Chronic-phase infection (2 to 16 weeks) is characterized by stable viable counts. (A) Static scenario. CMI halts bacterial replication after the acute phase of infection. Viable counts (CFU) (blue line) and total counts (CEQ) (red line) do not diverge over time. (B) Dynamic scenario. Bacterial replication continues at an undiminished rate (doubling time, 24.6 h) throughout the chronic phase, but bactericidal CMI kills 50% of the bacteria after each round of cell division. Balanced growth and death result in stable viable counts while total counts accumulate, resulting in rapid divergence of CEQ and CFU. (C and D) Semidynamic scenarios where the rate of bacterial cell division is reduced by 50% (C) or 90% (D) from the acute-phase rate, resulting in more-gradual divergence of CEQ and CFU.

MATERIALS AND METHODS

Static and dynamic models of host-pathogen equilibrium. A simple in silico model of in vivo bacterial growth dynamics and host-pathogen equilibrium was generated using Microsoft Excel (spreadsheet available upon request). The following input parameters were selected for generating the curves depicted in Fig. 1: inoculum, 200 CFU; acute phase, 0 to 2 weeks postinfection; chronic phase, 2 to 16 weeks postinfection; replication rate (population doubling time) during acute-phase growth, 24.6 h. These input parameters were selected in order to match the experimentally determined parameters shown in Fig. 2, but the model will accommodate any set of input parameters. In our model (see Fig. 1), the curves depicting viable CFU incorporate the potentially bactericidal impact of the immune response by calculating pre- and postkilling CFU values on a daily basis. Different types of equilibria (from fully static to fully dynamic or semidynamic scenarios) can be modeled by varying the growth rate and the killing rate during the chronic phase of infection; in our specific case, the chronic phase was defined as 2 to 16 weeks postinfection, although these parameters can also be varied as appropriate.

"Prekilling" CFU values (CFU_{pre}) on each successive day were calculated according to the formula $CFU_{pre} = CFU_i \cdot e^{K \cdot T}$, where CFU_i is the number of CFU on the preceding day (postkilling), K is the growth rate constant (per day) before adjustment for host-mediated killing, and time (T) is 1 day. "Postkilling" CFU values (CFU_{post}) on each successive day were calculated according to the formula $CFU_{post} = CFU_i \cdot e^{K' \cdot T}$, where CFU_i is the number of CFU on the preceding day (postkilling), K' is the growth rate constant (per day) after adjustment for immune-mediated killing, and T is 1 day. The "static" scenario (Fig. 1A) was modeled by setting K at 0 day^{-1} (doubling time, ∞) during the chronic phase of infection (2 to 16 weeks). The "dynamic" scenario (Fig. 1B) was modeled by setting K at 0.6764 day^{-1} (a 24.6-h doubling time, identical to the acute-phase rate). The "partially dynamic" scenarios, with bacterial cell division rates reduced by 50% (Fig. 1C) or 90% (Fig. 1D) from the acute-phase rate, were modeled by setting K at 0.3382 day^{-1} (49.2 h) or 0.0676 day^{-1} (246.0 h), respectively. For illustrative purposes, the curves in Fig. 1 were generated by setting K' to 0 during the chronic phase of infection (2 to 16 weeks) in order to maintain a stable plateau in CFU numbers; more-complex scenarios (rising or falling CFU over time) can be modeled by independently varying K and K' (as in Fig. 2).

Numbers of total CEQ (tCEQ) on each successive day were calculated by summing the CEQ from viable bacteria (vCEQ) with those from dead bacteria (dCEQ) according to the formula tCEQ = vCEQ + dCEQ, where vCEQ = CFU_{post} and dCEQ = $\Sigma(CFU_{pre} - CFU_{post})$ for each successive day inclusive of the current day. The chromosomal ploidy of *M. tuberculosis* under different growth conditions is unknown; in *M. tuberculosis*-infected mice, the experimentally determined bacterial CEQ/CFU ratio at 2 weeks postinfection is typically 1 to 3 (Fig. 2, 3, and 4; also our unpublished results). For illustrative purposes, a ploidy value of 2 was arbitrarily used to generate the curves in Fig. 1 in order to avoid overlap of the CFU and CEQ curves in Fig. 1A. The ploidy value was conservatively set at 1 for the modeled curves depicted in Fig. 2; higher ploidy values would lead to a more rapid divergence of the CEQ and CFU curves.

Mycobacteria and culture conditions. *M. tuberculosis* strains (Erdman and H37Rv) were propagated at 37°C either in Middlebrook 7H9 broth (Difco) containing 10% oleic acid-albumin-dextrose-catalase (Difco) and 0.05% Tween 80 (Sigma) or on Middlebrook 7H10 agar containing 10% oleic acid-albumin-dextrose-catalase. Cycloheximide (100 $\mu g\ ml^{-1}$) was included in the media to prevent fungal growth. Frozen stocks were prepared by growing bacteria in roller bottles in 7H9 broth to mid-log phase (optical density at 600 nm [OD_{600}], ~0.5), collecting cells by centrifugation, washing once with phosphate-buffered saline containing 0.05% Tween 80 (PBST), adding glycerol to 15%, and storing in aliquots at −80°C. Bacterial stocks were titered by plating PBST-diluted bacterial suspensions on 7H10 agar and scoring colonies after 3 to 4 weeks at 37°C.

Mouse infections and chemotherapy. C57BL/6J and gamma interferon-deficient (IFN-$\gamma^{-/-}$) mice, aged 5 to 10 weeks, were purchased from Jackson Laboratories. Mice were housed under specific-pathogen-free conditions at Rockefeller University; they were routinely tested and found to be free of common mouse pathogens. All experiments with live mice were performed in accordance with the National Institutes of Health Guidelines for the Care and Use of Laboratory Animals and were approved by Rockefeller University's Institutional Animal Care and Use Committee.

For intravenous infections, frozen aliquots of cells were thawed, diluted to ~10^7 CFU ml^{-1} in PBST, cup sonicated (40 s) to disperse clumps, and inoculated by injection of 0.1 ml (~10^6 CFU) of the bacterial suspension into a lateral tail vein. For respiratory infections, bacteria were grown in 7H9 broth to mid-log phase (OD_{600}, ~0.5), collected by centrifugation, washed once with PBST, and suspended at ~10^6 to 10^8 CFU ml^{-1} (adjusted by OD_{600}), depending on the dosage required (10^1 to 10^3 CFU per mouse); aerosol exposure of mice was

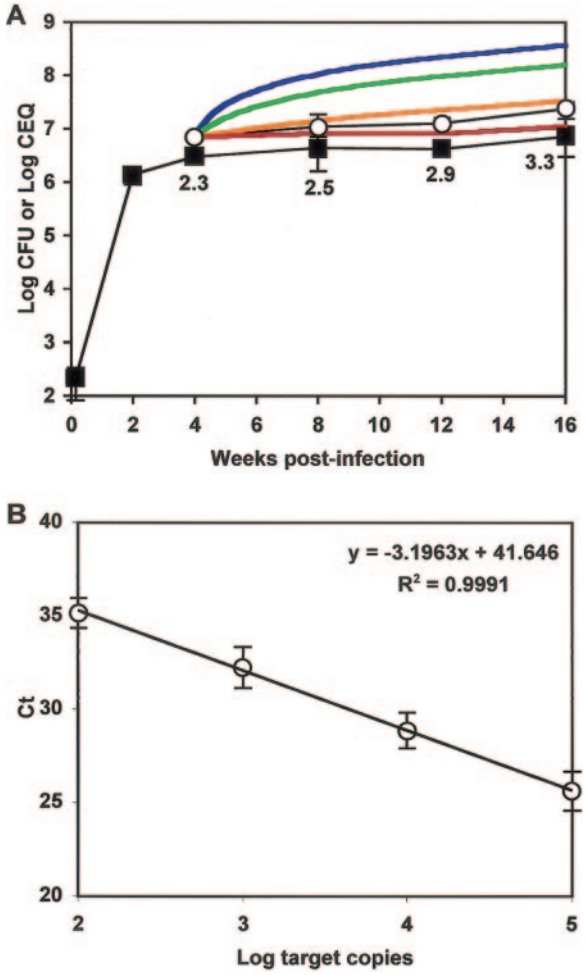

FIG. 2. Comparison of modeled and experimentally determined CFU and CEQ curves in mice. (A) C57BL/6 mice were aerosol infected with *M. tuberculosis* (~200 CFU per mouse). At 24 h and at 2, 4, 8, 12, and 16 weeks postinfection, groups of mice were sacrificed and lungs were removed. Viable counts (CFU) were quantified by plating serial dilutions of lung homogenates (filled squares); total counts (CEQ) were quantified by QPCR (open circles). Modeled CEQ values were derived by using the static (red line) or dynamic (blue line) equilibrium scenario, or a semidynamic scenario in which the rate of cell division during chronic infection was reduced by 50% (green line) or 90% (orange line) from the acute-infection rate. Symbols represent mean CFU or CEQ values ($n = 4$ mice per group); error bars, standard deviations. Numbers below curves indicate CEQ/CFU ratios at the corresponding time points. *P* values for pairwise comparisons of the experimental and modeled CEQ values at 16 weeks were as follows: for the experimental versus the dynamic or semidynamic (50%) scenario, $P < 0.001$; for the experimental versus the static or semidynamic (10%) scenario, $P > 0.05$. Results are representative of two experiments. (B) Standard curve for the *fadE15* primer-beacon set used to quantify bacterial CEQ in tissue homogenates. Ct values (*y* axis) were obtained by QPCR of 10^2, 10^3, 10^4, or 10^5 copies of the target DNA (*x* axis). Symbols (open circles) represent mean Ct values from three independent experiments where $n \geq 2$ replicates per experiment; error bars, standard deviations. The trend line drawn through the data points indicates the linear regression curve, which was calculated by using the least-squares method.

carried out for 15 min, followed by a 30-min purge with room air, by using a custom-built aerosol exposure chamber (University of Wisconsin, Madison), as described elsewhere (13, 30). At selected time points postinfection, mice ($n = 4$) were euthanized by CO_2 exposure, and lungs were removed for enumeration of bacterial CFU (left lung) and CEQ (right lung).

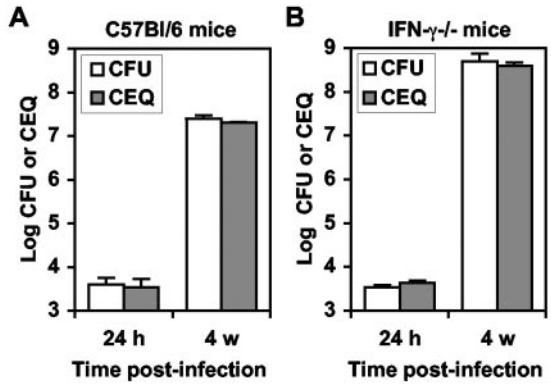

FIG. 3. Quantification of *M. tuberculosis* CEQ in mouse lungs is not limited by a detection ceiling at high bacterial loads. C57BL/6 mice (A) and IFN-$\gamma^{-/-}$ mice (B) were aerosol infected with *M. tuberculosis* (~4,000 CFU per mouse). At 24 h and 4 weeks (w) postinfection, mice were sacrificed and lungs were removed for analysis. Viable counts were quantified by plating serial dilutions of lung homogenates for CFU (open bars); total counts (CEQ) were quantified by QPCR (shaded bars). Bars represent mean CFU or CEQ values ($n = 4$ mice per group); error bars, standard deviations. This experiment was performed once.

Where indicated, *M. tuberculosis*-infected mice received INH (25 mg per kg of body weight per day), delivered ad libitum in the drinking water, starting at 4 weeks postinfection and continuing for 8 weeks.

Quantification of *M. tuberculosis* CFU. *M. tuberculosis* CFU was enumerated by homogenizing the left lung of each mouse in 5 ml of PBST by using a Polytron tissue homogenizer, plating the diluted homogenates on 7H10 agar, and scoring colonies after 3 to 4 weeks at 37°C.

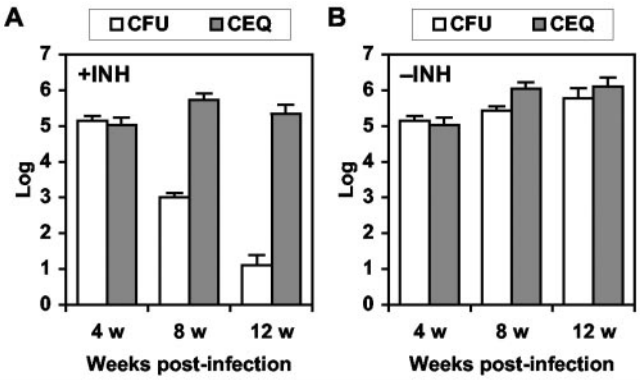

FIG. 4. Chromosomes of nonviable *M. tuberculosis* in mouse lungs are not removed or degraded rapidly. C57BL/6 mice were infected intravenously with *M. tuberculosis* (~10^6 CFU per mouse). One group (A) received INH (25 mg kg^{-1} day^{-1}) for 8 weeks starting at 4 weeks postinfection; a control group (B) was left untreated. At 4, 8, and 12 weeks postinfection, mice from INH-treated and untreated groups were sacrificed and lungs were removed. Viable counts (CFU) were quantified by plating serial dilutions of lung homogenates (open bars); total counts (CEQ) were quantified by QPCR (shaded bars). Bars represent mean CFU or CEQ values ($n = 4$ mice per group); error bars, standard deviations from the means. In pairwise comparisons of CFU values in the INH-treated group for 4 versus 8 weeks or 4 versus 12 weeks postinfection, differences were highly significant ($P < 0.005$). In pairwise comparisons of CEQ values in the INH-treated group for 4 versus 8 weeks or 4 versus 12 weeks postinfection, differences were not significant ($P > 0.05$). Results are representative of two experiments.

Quantification of *M. tuberculosis* CEQ. *M. tuberculosis* chromosomal DNA was prepared by homogenizing the right lung of each mouse in 5 ml of PBST, collecting the bacteria by centrifugation at 3,000 × *g* for 10 min at 4°C, resuspending the bacterial pellet in 1 ml of Tris-EDTA, adding 0.25 ml of warm (70°C) phenol-chloroform–isoamyl alcohol (25:24:1) (Sigma) and 0.25 ml of zirconia-silica beads (Biospec Products), and breaking the bacteria in a bead beater (Biospec Products). Cell debris was removed by centrifugation at 12,000 × *g* for 10 min, 50 μl of 5 M NaCl was added to the clarified supernatant, extraction with phenol-chloroform–isoamyl alcohol was repeated, and genomic DNA was precipitated by addition of isopropanol. The precipitated genomic DNA from a single infected mouse was ethanol washed, air dried, resuspended in 300 μl of water, and stored at −20°C. Quantitative real-time PCRs (QPCRs) were carried out as described previously (14, 32). Each reaction was in a volume of 50 μl containing 1× Taqman buffer A (Perkin-Elmer), 4 mM $MgCl_2$, 0.25 mM deoxynucleoside triphosphates, 2.5 U of AmpliTaq Gold polymerase (Perkin-Elmer), 0.5 μM *fadE15* primers, 0.3 μM *fadE15* molecular beacon, and template DNA. Typically, 1 to 2 μl of template DNA (representing 0.33 to 0.67% of the total genomic DNA extracted from a single mouse) was used per reaction. In some cases (where bacterial loads were very high), template DNAs were diluted before amplification in order to obtain QPCR threshold cycle (Ct) values in the range of 25 to 35; control reactions confirmed that dilution of the template had no effect on the linearity of amplification (data not shown).

The set of primers and the molecular beacon used to quantify bacterial chromosomes had the following sequences (hybridizing to sequences in the *fadE15* gene): FAM-GGGCCTTCGGACTTCGTCTCCTTCAGGCCC (molecular beacon), GCGGGTCGGGCTGGTCAAC (forward primer), and CCTCGCCCAT GATGGTAGGAAC (reverse primer). Real-time QPCRs were run and analyzed on an ABI 7900 machine according to the manufacturer's instructions. PCR conditions were as follows: an Amplitaq Gold activation step at 95°C (10 min), followed by 40 cycles of 95°C (30 s), 57°C (30 s; data collection), and 72°C (30 s). Standard curves were generated by using serial dilutions of *M. tuberculosis* genomic DNA of known concentration. Quantitative analysis of the data was carried out as described elsewhere (14, 32).

Statistical analysis. Student's *t* test (two tailed) was used to evaluate differences in bacterial CFU and CEQ obtained from infected mouse lungs or from in silico modeling. Data are represented as means; error bars indicate standard deviations from the means. Trend lines were computed by using the least-squares method.

RESULTS

Modeling the host-pathogen equilibrium in chronically infected mice. In the mouse model of TB, the chronic phase of infection is characterized by progressive lung pathology despite relatively stable numbers of viable bacteria enumerated as CFU (25). The plateau in the bacterial growth curve could represent a "static" equilibrium, in which the rate of bacterial cell division is very slow, or a "dynamic" equilibrium, in which rapid bacterial cell division continues unabated, balanced by an equal rate of bacterial death effected by host immune mechanisms (24). The latter scenario would be akin to the highly dynamic equilibrium observed in human immunodeficiency virus (HIV) infection prior to the onset of AIDS (29). We reasoned that the two scenarios—static versus dynamic—could be distinguished by comparing the "viable counts" (bacterial CFU) and "total counts" (bacterial CEQ) at various stages in chronically infected animals. The static model predicts that CFU and CEQ will not diverge over time, whereas the dynamic model predicts that bacterial CEQ will accumulate over time while CFU will remain stable. To illustrate these alternative scenarios, we devised a simple in silico model that can be used to generate CFU and CEQ curves representing a static equilibrium in which CMI is strictly bacteriostatic (Fig. 1A), or a dynamic equilibrium in which CMI is strictly bactericidal (Fig. 1B). The model can also be used to generate semidynamic scenarios in which CMI exerts both bacteriostatic and bactericidal effects, resulting in a net reduction in the bacterial population growth rate during the persistent phase of infection (Fig. 1C and D). The derivation of our model is described in Materials and Methods.

In the "static" scenario, the model predicted that both viable counts (CFU) and total counts (CEQ) would remain stable and would not diverge over time (Fig. 1A). In the "dynamic" scenario, the model predicted that although viable counts would remain stable over time, total counts would gradually rise due to the accumulation of dead bacteria; in the modeled experiment for which results are shown in Fig. 1B, the CEQ/CFU ratio increased ~100-fold between 2 and 16 weeks postinfection. We also modeled semidynamic scenarios where CMI exerted both bacteriostatic and bactericidal effects, resulting in stable numbers of CFU but gradual accumulation of CEQ. The semidynamic scenarios could reflect either a partial effect of CMI on the entire bacterial population or variable efficacy of CMI against different bacterial subpopulations (Fig. 1C and D); our model cannot distinguish between these possibilities. The semidynamic scenarios were modeled by varying the rate of bacterial cell division and death during the chronic phase, as described in Materials and Methods. When the rate of cell division during the chronic phase was reduced by 50% (Fig. 1C) or 90% (Fig. 1D) from the cell division rate during the acute phase, the CEQ/CFU ratio nonetheless rose appreciably (~40- or ~8-fold, respectively) between 2 and 16 weeks postinfection. Our model will also accommodate more-complex scenarios, such as fluctuating rates of cell division or cell death during the course of infection (see Fig. 2). A key assumption is that nonviable bacteria (and their chromosomes) are not removed or degraded over time; here we provide experimental support for this assumption (see below), in agreement with evidence previously adduced by others (24).

Comparison of modeled and experimentally determined CFU and CEQ curves in mice. In order to generate experimental values for bacterial CFU and CEQ during the course of chronic murine infection, C57BL/6 mice were aerosol infected with ~200 CFU of *M. tuberculosis* Erdman and groups were sacrificed at selected time points for quantitative analysis of bacillary numbers in the lungs. Viable counts (CFU) were enumerated by plate culture of lung homogenates; total counts (CEQ) were enumerated by use of QPCR, as described in Materials and Methods.

During the acute phase of infection (0 to 2 weeks postinfection), viable counts in the lungs increased exponentially, with an average population doubling time of 24.6 h (Fig. 2). During the chronic phase of infection (4 to 16 weeks postinfection), there was a much slower rise in viable counts, with an average population doubling time of 1,676 h (~70 days) (Fig. 2). The CEQ/CFU ratio showed little change during the chronic phase of infection (Fig. 2), indicating that there was minimal accumulation of chromosomes representing dead bacteria. These observations resemble the predicted curves generated by the static scenario in our model (Fig. 1A) and differ markedly from the curves generated by the dynamic scenario (Fig. 1B), thus supporting the idea that the rate of bacterial cell division is very low during the chronic phase of infection.

In order to provide a more direct comparison between our modeled and experimental results, we modeled the dynamic and static scenarios using the growth rate constants derived from the experimental data depicted in Fig. 2, taking into

account any changes in bacterial CFU between time points by varying the growth rate constants (*K* values) appropriately. The experimentally determined CEQ values diverged sharply from the modeled CEQ values in the dynamic scenario and from those in the semidynamic scenario where bacterial replication during the chronic phase was reduced by 50%, and they fell between the modeled CEQ values for the static scenario and those for the semidynamic scenario where bacterial replication during the chronic phase was reduced by 90% (Fig. 2). The parallel rise in experimental CFU and CEQ values between 2 and 16 weeks postinfection indicates that stasis is not absolute, although the doubling time of the bacterial population during the chronic phase is increased nearly 70-fold (1,676 h) over that in the acute phase (24.6 h). Thus, although it is likely that bacterial growth continues at a reduced rate during the chronic phase of infection, our results are not consistent with a model in which rapid bacterial cell division is balanced by equally rapid cell death.

Large numbers of bacterial chromosomes can be quantified in mouse lungs. We considered the possibility that our inability to detect a divergence of CFU and CEQ during the chronic phase of infection might be due to technical limitations in our methods for extraction and quantification of bacterial chromosomes from infected lungs. In order to confirm that there was no ceiling on the number of chromosomes per lung that we could accurately quantify, we enumerated CFU and CEQ in aerosol-infected IFN-γ-deficient mice, which are unable to control replication of *M. tuberculosis* in the lungs (3, 8). By 4 weeks postinfection, shortly before the IFN-$\gamma^{-/-}$ mice became moribund, the bacterial load in the lungs had reached $\sim 10^9$ CFU per mouse; the number of CEQ detected by QPCR corresponded very closely to the number of CFU detected by plate culture (Fig. 3B). Close correspondence of CFU and CEQ was also observed in immunocompetent C57BL/6 mice infected in parallel, although the numbers were much lower than those in the IFN-γ-deficient mice (Fig. 3A). The close correspondence of CFU and CEQ spanning a range of >5 $\log_{10}$ units confirms that our inability to detect a divergence of bacterial CFU and CEQ trajectories in chronically infected mice (Fig. 2) was not due to a technical limitation of the QPCR assay.

Persistence of dead bacteria in mouse lungs. We considered the possibility that our inability to detect substantial accumulation of bacterial chromosomes during the chronic phase of infection might be due to rapid removal or degradation of killed bacteria. This issue was addressed in an earlier study (24), where it was shown that microscopically visible AFB in the lungs persisted in relatively stable numbers for several months despite the elimination of CFU by treatment of mice with antimycobacterial drugs. In order to address this issue by using QPCR to quantify bacterial chromosomes in the lungs, we assessed the impact of INH therapy on viable (CFU) and total (CEQ) bacterial counts in chronically infected C57BL/6 mice. Untreated controls showed relatively stable viable and total counts between 4 and 12 weeks postinfection (Fig. 4B). In contrast, mice treated with INH for 8 weeks (from 4 to 12 weeks postinfection) showed marked reductions in viable counts (3.6 $\log_{10}$ units), whereas total counts remained stable (Fig. 4A). These observations confirm that nonviable tubercle bacilli (and their chromosomes) are not subject to rapid removal or degradation, in agreement with previous results from other groups (5, 24). However, we cannot rule out the possibility that the chromosomes of bacteria that are killed by host immune mechanisms are rapidly degraded, whereas the chromosomes of bacteria that are killed by antimicrobial agents are not. Our results also do not rule out the possibility that the stable number of viable counts in the lungs of chronically infected mice is due to replication in situ balanced by trafficking of organisms out of the lungs, resulting in failure of both CFU and CEQ to accumulate over time.

DISCUSSION

A key question in the context of any persistent infection is the replication status of the pathogen over time. Dynamic pathogens—examples include HIV and hepatitis C virus—replicate at very high rates throughout the course of infection. In individuals persistently infected with HIV or hepatitis C virus, a dynamic equilibrium is achieved in which a relatively stable viral load is maintained by balanced production and immune-mediated destruction of virions (23, 29). Viral persistence is also facilitated by antigenic variation, involving sequential emergence of variants that temporarily escape surveillance by the adaptive immune response. Antigenic variation is an essential persistence strategy of many slower-replicating pathogens as well, including parasites and bacteria; well-characterized examples include African trypanosomes and *Borrelia* spp. (4). These pathogens display oscillating population kinetics in vivo, representing sequential waves of antigenic variants that (temporarily) escape destruction by the adaptive immune response. Although antigenic variation is a common feature of many persistent pathogens, there is little evidence to support a role for antigenic variation in *M. tuberculosis* persistence in chronically infected individuals (2). We propose that *M. tuberculosis* represents a third persistence strategy, where exponential replication of the organism during the acute phase of infection is followed by a relatively static equilibrium, a state of slow-replicating or nonreplicating persistence, during the chronic phase.

The hypothesis that persistent mycobacteria are in a slow-replicating or nonreplicating state is consistent with several observations: (i) induction of a gene expression program that is characteristic of nonreplicating bacilli during the chronic phase of murine infection (28), (ii) the relatively poor efficacy of drugs that target cell wall synthesis (such as INH) when administered to chronically infected mice compared to acutely infected mice (15), (iii) the increased thermal stress resistance of *M. tuberculosis* (characteristic of stationary-phase cells) in chronically infected mice compared to acutely infected mice (34), (iv) the lack of accumulation of microscopically visible AFB in chronically infected mice (24), and (v) the lack of accumulation of bacterial chromosomes in chronically infected mice (described here). Kanai (11) provided direct proof of the ability of nonreplicating *M. tuberculosis* to persist in vivo, by showing that continued administration of streptomycin was not necessary for persistence of a streptomycin-dependent strain of *M. tuberculosis* in chronically infected mice.

The ability of *M. tuberculosis* to persist without replicating does not imply that bacterial replication is entirely absent in chronically infected individuals or animals, nor does it imply that persistent bacteria are metabolically inactive. Indeed, slow fluctuations in the bacterial load over time, which are typically observed in chronically infected mice, presumably reflect slow or

intermittent replication of at least some bacilli (27), and the dramatic increase in bacterial load in late-stage infected mice (22) can be explained only in terms of bacterial replication. Evidence from the *Mycobacterium marinum*-leopard frog model also supports the idea that chronic mycobacterial infections involve some ongoing bacterial cell division (1). What seems increasingly likely, however, is that *M. tuberculosis* persistence in chronically infected mice does not represent a highly dynamic equilibrium in which rapid bacterial growth is balanced by equally rapid immune-mediated killing, but rather a relatively static equilibrium in which the rate of bacterial cell division is very low. It is not known to what extent this conclusion can be extrapolated to humans with chronic TB or latent TB infection. Studies on TB lesions in humans suggest that the replicative state of the bacteria may differ depending on the histopathological characteristics of the individual lesions (12, 33, 35).

The replicative and metabolic status of persistent bacilli has important implications for the development of more-effective interventions against persistent *M. tuberculosis* infections. Treatment of TB is notoriously difficult and protracted, requiring a minimum of 6 to 9 months of multidrug therapy to prevent post-therapy relapse (7). Most of the drugs currently used to treat TB are known to target cellular processes involved in cell growth, such as cell wall biogenesis and DNA replication; consequently, these drugs are less effective against bacteria that are not undergoing rapid cell division (17, 19, 31). Elucidation of the mechanisms required for persistence of *M. tuberculosis* in a slow-replicating or nonreplicating state in chronically infected individuals might suggest new strategies for targeting persistent bacteria.

ACKNOWLEDGMENTS

E.J.M.-E. was supported by a Robert D. Watkins predoctoral fellowship (American Society for Microbiology). J.D.M. acknowledges support from the Sequella Global Tuberculosis Foundation, the Ellison Medical Foundation, the Sinsheimer Fund, and the Irma T. Hirschl Trust. This work was funded by National Institutes of Health grant AI051702 (to J.D.M.).

REFERENCES

1. **Bouley, D. M., N. Ghori, K. L. Mercer, S. Falkow, and L. Ramakrishnan.** 2001. Dynamic nature of host-pathogen interactions in *Mycobacterium marinum* granulomas. Infect. Immun. **69:**7820–7831.
2. **Cole, S. T.** 2002. Comparative and functional genomics of the *Mycobacterium tuberculosis* complex. Microbiology **148:**2919–2928.
3. **Cooper, A. M., D. K. Dalton, T. A. Stewart, J. P. Griffin, D. G. Russell, and I. M. Orme.** 1993. Disseminated tuberculosis in interferon γ gene-disrupted mice. J. Exp. Med. **178:**2243–2247.
4. **Deitsch, K. W., E. R. Moxon, and T. E. Wellems.** 1997. Shared themes of antigenic variation and virulence in bacterial, protozoal, and fungal infections. Microbiol. Mol. Biol. Rev. **61:**281–293.
5. **de Wit, D., M. Wootton, J. Dhillon, and D. A. Mitchison.** 1995. The bacterial DNA content of mouse organs in the Cornell model of dormant tuberculosis. Tuber. Lung Dis. **76:**555–562.
6. **Dye, C., S. Scheele, P. Dolin, V. Pathania, and M. C. Raviglione.** 1999. Consensus statement. Global burden of tuberculosis: estimated incidence, prevalence, and mortality by country. WHO Global Surveillance and Monitoring Project. JAMA **282:**677–686.
7. **El-Sadr, W. M., D. C. Perlman, E. Denning, J. P. Matts, and D. L. Cohn.** 2001. A review of efficacy studies of 6-month short-course therapy for tuberculosis among patients infected with human immunodeficiency virus: differences in study outcomes. Clin. Infect. Dis. **32:**623–632.
8. **Flynn, J. L., J. Chan, K. J. Triebold, D. K. Dalton, T. A. Stewart, and B. R. Bloom.** 1993. An essential role for interferon γ in resistance to *Mycobacterium tuberculosis* infection. J. Exp. Med. **178:**2249–2254.
9. **Flynn, J. L., and J. Chan.** 2001. Tuberculosis: latency and reactivation. Infect. Immun. **69:**4195–4201.
10. **Flynn, J. L., and J. Chan.** 2001. Immunology of tuberculosis. Annu. Rev. Immunol. **19:**93–129.
11. **Kanai, K.** 1966. Experimental studies on host-parasite equilibrium in tuberculosis infection, in relation to vaccination and chemotherapy. Jpn. J. Med. Sci. Biol. **19:**181–199.
12. **Kaplan, G., F. A. Post, A. L. Moreira, H. Wainwright, B. N. Kreiswirth, M. Tanverdi, B. Mathema, S. V. Ramaswamy, G. Walther, L. M. Steyn, C. E. Barry III, and L.-G. Bekker.** 2003. *Mycobacterium tuberculosis* growth at the cavity surface: a microenvironment with failed immunity. Infect. Immun. **71:**7099–7108.
13. **MacMicking, J. D., G. A. Taylor, and J. D. McKinney.** 2003. Immune control of tuberculosis by IFN-γ-inducible LRG-47. Science **302:**654–659.
14. **Manganelli, R., E. Dubnau, S. Tyagi, F. R. Kramer, and I. Smith.** 1999. Differential expression of 10 sigma factor genes in *Mycobacterium tuberculosis*. Mol. Microbiol. **31:**715–724.
15. **McCune, R. M., R. Tompsett, and W. McDermott.** 1956. Fate of *Mycobacterium tuberculosis* in mouse tissues as determined by the microbial enumeration technique. II. The conversion of tuberculous infection to the latent state by the administration of pyrazinamide and a companion drug. J. Exp. Med. **104:**763–801.
16. **McDermott, W.** 1958. Microbial persistence. Yale J. Biol. Med. **30:**257–291.
17. **McKinney, J. D.** 2000. *In vivo veritas*: the search for TB drug targets goes live. Nat. Med. **6:**1330–1333.
18. **Middlebrook, G.** 1952. Sterilization of tubercle bacilli by isonicotinic acid hydrazide and the incidence of variants resistant to the drug *in vitro*. Am. Rev. Tuberc. Pulm. Dis. **65:**765–767.
19. **Mitchison, D. A.** 2004. The search for new sterilizing anti-tuberculosis drugs. Front. Biosci. **9:**1059–1072.
20. **Muñoz-Elías, E. J., and J. D. McKinney.** 2002. Bacterial persistence: strategies for survival, p. 331–355. *In* S. H. E. Kaufmann, A. Sher, and R. Ahmed (ed.), Immunology of infectious diseases. ASM Press, Washington, D.C.
21. **North, R. J., and Y. J. Jung.** 2004. Immunity to tuberculosis. Annu. Rev. Immunol. **22:**599–623.
22. **Orme, I. M.** 1988. A mouse model of the recrudescence of latent tuberculosis in the elderly. Am. Rev. Respir. Dis. **137:**716–718.
23. **Pawlotsky, J.-M.** 2004. Pathophysiology of hepatitis C virus infection and related liver disease. Trends Microbiol. **12:**96–102.
24. **Rees, R. J. W., and P. D. Hart.** 1961. Analysis of the host-parasite equilibrium in chronic murine tuberculosis by total and viable bacillary counts. Br. J. Exp. Pathol. **42:**83–88.
25. **Rhoades, E. R., A. A. Frank, and I. M. Orme.** 1997. Progression of chronic pulmonary tuberculosis in mice aerogenically infected with virulent *Mycobacterium tuberculosis*. Tuber. Lung Dis. **78:**57–66.
26. **Seiler, P., T. Ulrichs, S. Bandermann, L. Pradl, S. Jorg, V. Krenn, L. Morawietz, S. H. Kaufmann, and P. Aichele.** 2003. Cell-wall alterations as an attribute of *Mycobacterium tuberculosis* in latent infection. J. Infect. Dis. **188:**1326–1331.
27. **Sever, J. L., and G. P. Youmans.** 1957. Enumeration of viable tubercle bacilli from the organs of nonimmunized and immunized mice. Am. Rev. Tuberc. Pulm. Dis. **76:**616–635.
28. **Shi, L., Y. J. Jung, S. Tyagi, M. L. Gennaro, and R. J. North.** 2003. Expression of Th1-mediated immunity in mouse lungs induces a *Mycobacterium tuberculosis* transcription pattern characteristic of nonreplicating persistence. Proc. Natl. Acad. Sci. USA **100:**241–246.
29. **Simon, V., and D. D. Ho.** 2003. HIV-1 dynamics in vivo: implications for therapy. Nat. Rev. Microbiol. **1:**181–190.
30. **Smith, D. W., D. N. McMurray, E. H. Wiegeshaus, A. A. Grover, and G. E. Harding.** 1970. Host-parasite relationships in experimental airborne tuberculosis. IV. Early events in the course of infection in vaccinated and nonvaccinated guinea pigs. Am. Rev. Respir. Dis. **102:**937–949.
31. **Stewart, G. R., B. D. Robertson, and D. B. Young.** 2003. Tuberculosis: a problem with persistence. Nat. Rev. Microbiol. **1:**97–105.
32. **Timm, J., F. A. Post, L.-G. Bekker, G. B. Walther, H. C. Wainwright, R. Manganelli, W.-T. Chan, L. Tsenova, B. Gold, I. Smith, G. Kaplan, and J. D. McKinney.** 2003. Differential expression of iron-, carbon-, and oxygen-responsive mycobacterial genes in the lungs of chronically infected mice and tuberculosis patients. Proc. Natl. Acad. Sci. USA **100:**14321–14326.
33. **Vandiviere, H. M., W. E. Loring, I. Melvin, and S. Willis.** 1956. The treated pulmonary lesion and its tubercle bacillus. II. The death and resurrection. Am. J. Med. Sci. **232:**30–37.
34. **Wallace, J. G.** 1961. The heat resistance of tubercle bacilli in the lungs of infected mice. Am. Rev. Respir. Dis. **83:**866–871.
35. **Wayne, L. G., and D. Salkin.** 1956. The bacteriology of resected tuberculous pulmonary lesions. Am. Rev. Tuberc. Pulm. Dis. **74:**376–387.
36. **Young, D., T. Hussell, and G. Dougan.** 2002. Chronic bacterial infections: living with unwanted guests. Nat. Immunol. **3:**1026–1032.

Editor: S. H. E. Kaufmann